New gravity-derived bathymetry for the Thwaites, Crosson and Dotson ice shelves revealing two ice shelf populations

Tom A. Jordan[1], David Porter[2], Kirsty Tinto[2], Romain Millan[3], Atsuhiro Muto[4], Kelly Hogan[1], Robert D. Larter[1], Alastair G.C. Graham[5], John D. Paden[6]

5   [1] British Antarctic Survey, High Cross, Madingley Road, Cambridge, CB3 0ET, UK
[2] Lamont Doherty Earth Observatory
[3] Institut des Géosciences de l'Environnement, Université Grenoble Alpes, CNRS, 38000 Grenoble, France
[4] Dept. of Earth and Environmental Science, Temple University, Philadelphia, PA 19122, USA
[5] College of Marine Science, University of South Florida, St Petersburg, FL 33701, USA.
10   [6] Center for Remote Sensing of Ice Sheets (CReSIS), The University of Kansas, Kansas 66045, USA

Correspondence to: Tom A. Jordan (tomj@bas.ac.uk)

Abstract. Ice shelves play a critical role in the long-term stability of ice sheets through their buttressing effect. The underlying bathymetry and cavity thickness are key inputs for modelling future ice sheet evolution. However, direct observation of sub-ice shelf bathymetry is time consuming, logistically risky, and in some areas simply not possible. Here we use airborne gravity

15   anomaly data to provide new estimates of sub-ice shelf bathymetry outboard of the rapidly changing West Antarctic Thwaites Glacier, and beneath the adjacent Dotson and Crosson Ice Shelves. This region is of especial interest as the low-lying inland reverse slope of the Thwaites glacier system makes it vulnerable to marine ice sheet instability, with rapid grounding-line retreat observed since 1993 suggesting this process may be underway. Our results confirm a major marine channel >800 m deep extends to the front of Thwaites Glacier, while the adjacent ice shelves are underlain by more complex bathymetry.

20   Comparison of our new bathymetry with ice shelf draft reveals that ice shelves formed since 1993 comprise a distinct population where the draft conforms closely to the underlying bathymetry, unlike the older ice shelves which show a more uniform depth of the ice base. This indicates that despite rapid basal melting in some areas, these "new" ice shelves are not yet in equilibrium with the underlying ocean system. We propose qualitative models of how this transient ice-shelf configuration may have developed.

25   **1 Introduction**

The Thwaites Glacier system is a globally important region of change in the cryosphere system (Fig. 1a) (Scambos et al., 2017). In this region the marine based West Antarctic Ice Sheet comes into direct contact with upwelling modified Circumpolar Deep Water (mCDW) which is warm relative to the typical cool dense shelf water (Jenkins et al., 2018). This warm water can both erode the buttressing ice shelves, and directly melt the grounded ice, both factors driving dynamic thinning and retreat of

30   glaciers and contributing to rising global sea level (Pritchard et al., 2012). The inland reverse slope of the bed beneath Thwaites Glacier and some of the adjacent glaciers means that marine ice sheet instability may occur (Schoof, 2007;Weertman, 1974).

In this case a feedback is setup where grounding line retreat exposes a progressively larger cross-sectional area of ice, hence more ice fluxes into the ocean leading to further glacial retreat. Satellite observations revealing an increase in the velocity of ~100 ma^{-1} extending ~100 km inland from the Thwaites grounding line and surface draw down of over 1 ma^{-1} indicate that

35   this region is changing now (Gardner et al., 2018;Milillo et al., 2019). It has been argued that dramatic retreat of the grounding lines of Thwaites, Pope, Smith and Kohler glaciers of between 10 and 30 km since 1993 (Fig. 1a) means that ice sheet collapse due to marine ice sheet instability may have begun (Rignot et al., 2014;Milillo et al., 2019).

Understanding the sub-ice-shelf bathymetry beneath the ice shelves separating the open marine realm of the Amundsen Sea Embayment and the grounded ice of the Thwaites Glacier system is of particular importance for the evolution of this region

40   (Fig. 1a). The bathymetry beneath ice shelves is a fundamental control on the ice sheet stability as the shape of the water cavity is a first order control on sub-ice shelf currents, including the flux of warm, deep ocean water to the ice shelf bases and the grounding line beyond (Jacobs et al., 2011). Melting, thinning and ultimately disintegration of ice shelves will trigger faster glacial flow, forcing glacial retreat, leading to global mean sea level rise (Scambos et al., 2004;Rignot et al., 2014). Cavity shape is also likely an important factor controlling the rate of melting close to the grounding line (Milillo et al., 2019;Schoof,

45   2007). Direct measurements of sub-ice-shelf bathymetry by seismic spot measurements is slow and often impractical due to the extremely crevassed environment (Brisbourne et al., 2014;Rosier et al., 2018). Exploration of sub-ice-shelf cavities using autonomous underwater vehicles can also be risky and time consuming to attain regional coverage (Jenkins et al., 2010;Davies et al., 2017). An alternative technique to provide a first-order estimate of the bathymetry is the inversion of airborne gravity anomaly data, which can be collected quickly and efficiently over large areas.

50   Recovery of bathymetry from gravity data relies on the fundamental fact that the density contrast at the sea bed gives rise to significant and measurable gravity anomalies. A variety of techniques have been employed to invert gravity data for bathymetry. In the simplest case, the free-air anomaly is transformed directly to an equivalent bathymetric surface, typically using a fast Fourier transform approach such as the Parker–Oldenburg iterative method (Gómez-Ortiz and Agarwal, 2005), as applied to the Larsen Ice Shelf (Cochran and Bell, 2012). However, subsequent seismic observations indicate that, although

55   the broad pattern of the bathymetry was resolved, this approach can give rise to significant errors, attributed to geological factors such as crustal thickness and sedimentary basins distorting the gravity field (Brisbourne et al., 2014). An alternative technique models the bathymetry using gravity data along multiple 2D profiles, for example across the Abbot Ice Shelf (Cochran et al., 2014) and outboard of Thwaites Glacier (Tinto and Bell, 2011;Tinto et al., 2011). Such models are constrained to match known topography and inferences about the underlying geology provide additional constraints. The 3D bathymetry

60   beneath the Pine Island Glacier ice shelf was inverted from gravity data using a 3D prism model and a simulated annealing technique solving for bathymetry and a sedimentary layer (Muto et al., 2016). Although this technique returns a bathymetry model constrained by observations, it is not clear whether signatures due to sediments and bathymetry can be reliably separated without *a priori* constraints such as seismic observations (Roy et al., 2005). More recently, a 3D model constrained by regional bathymetry and subglacial topography was used to model bathymetry offshore of Pine Island and Thwaites glaciers, and

65   beneath the Crosson and Dotson Ice Shelves (Millan et al., 2017). This model showed a complex topography with deep

channels extending to the margin of the ice sheet, particularly in the Dotson-Crosson area where previously-unknown deep (>1200 m) channels were identified.

In this paper we re-evaluate the sub-ice-shelf bathymetry offshore from Thwaites Glacier and beneath the Crosson and Dotson Ice Shelves (Fig. 1a) through the integration of new airborne gravity data from the NERC/NSF International Thwaites Glacier

70   Collaboration (ITGC), Operation IceBridge (OIB) (Cochran and Bell, 2010, updated 2018) and new marine gravity data from the R/V Nathaniel B. Palmer collected during the cruise NBP19-02 (Fig. 1b). To recover bathymetry from gravity beneath the ice shelves we employ an algorithm-based approach similar to that used for the Brunt Ice Shelf (Hodgson et al., 2019). This approach constrains the recovered topography to match all direct topographic observations. This constraint helps account for geological factors such as variations in crustal thickness, sedimentary basins or intrusions. We acknowledge that away from

75   direct topographic observations the uncertainties in the bathymetric estimate due to geological factors increase. However, we suggest that using a well-constructed gravity-derived bathymetry is preferable to unconstrained interpolation across sub-ice-shelf bathymetric data gaps many 10s of kilometres wide. Such use of gravity data is routine for predicting topography in un-surveyed parts of the ocean using satellite data (Smith and Sandwell, 1994) and is being used in the Arctic where higher resolution airborne data are included (Abulaitijiang et al., 2019).

80   Our results confirm the shape and position of the previously identified troughs (Millan et al., 2017). Differences in the inversion results beneath the inboard parts of some of the ice shelves are identified, reflecting the higher resolution of the new gravity data set and differences in the methods used. Our improved topographic estimate reveals variations in sub-ice-shelf cavity thickness, which have implications for the rate at which the warm ocean water can access the present-day grounding lines, and the mechanism of grounding line retreat in these and other areas.

85

2 Methods

2.1 The integrated gravity and topographic data sets

We utilise airborne gravity data from OIB and the ITGC campaign, together with marine gravity data from cruise NBP19-02 (Fig. 1b and c). The OIB free-air gravity data has an error of ~1.67 mGal in this region and resolves anomalies with a ~10 km

90   full wavelength (Cochran and Bell, 2010, updated 2018;Tinto and Bell, 2011). The ITGC campaign utilised a 'strapdown' gravity approach (Becker et al., 2015;Wei and Schwarz, 1998), resulting in data with an internal error from crossover analysis of 1.56 mGal and resolving wavelengths down to ~5 km (see supplementary data Section S2). Airborne data were restricted to lines flown at <1500 m above the surface. Of this subset over 95% of the data were collected at 450 m ±200 m above the surface. Upward and downward continuation of the gravity data to a common altitude was neglected as continuation by ~200

95   m will have little impact given the ~1000 m range to the key bathymetric sources. Downward continuation can also introduce unnecessary artefacts and neglecting upward continuation preserves short wavelength gravity information. Marine gravity data from cruise NBP19-02 matched the pattern of the airborne anomalies, but was offset by 7.14 mGal. The majority of this offset is due to the difference between geoid (marine) and ellipsoid (airborne) references used for the different systems. In the area

of overlap the geoid-ellipsoid difference results in a ~9 mGal discrepancy, based on the GOCO3s satellite gravity model (Pail
100   et al., 2010). The residual ~ 2 mGal difference may reflect drift in the marine system, and potential discrepancies in base station
ties between the different surveys. The measured shift was removed from the marine line data as a DC value as the variation
in geoid-ellipsoid discrepancy in the overlap area is <0.1 mGal. All line data were then merged into a single database,
interpolated onto a 1 km mesh raster and filtered with a 5 km low pass filter removing residual line to line noise. This filter
wavelength is justified as anomalies with wavelengths <5 km are not expected to be resolved by the airborne gravity systems
105   used. The final, integrated free-air gravity map (Fig. 1c) shows a clear pattern of high and low anomalies, which to first order
match the main 5-10 km wavelength features visible in the available onshore subglacial topography and offshore bathymetry
(Fig. 1d).

The topographic observations onshore were taken from OIB line radar data (Paden et al., 2010, updated 2018), augmented
with new depth sounding radar collected along with the gravity data during the ITGC campaign. This new bed elevation data
110   was collected using a 550-900 MHz accumulation radar provided by the Center for Remote Sensing of Ice Sheets (CReSIS).
Bed elevations were picked from SAR processed radargrams in a semi-automated fashion. Although the primary target of this
radar system was shallow ice sheet structures bed elevation was resolved through ice up to ~1900 m thick. Visual inspection
revealed a few incorrect onshore bed picks in the OIB dataset on Bear Island, which gave bed elevations above the highly
accurate REMA surface digital elevation model (DEM) (Howat et al., 2019). These points were deleted from the integrated
115   bed elevation dataset. The line bed elevation data were corrected to the GL04c Geoid (Forste et al., 2008), and the data
interpolated onto a 1 km mesh raster. This gridded dataset was carefully masked to remove regions which are now covered by
the floating ice shelf based on the most up to date grounding lines (Rignot et al., 2014;Milillo et al., 2019). Bed elevation
values over local sub-shelf pinning points were also excluded. This masking mitigates the risk of the base of a floating ice
shelf being misidentified as a bed elevation point and biasing the inversion. Beyond the ice shelves we took the values
120   constrained by a new compilation of shipborne multibeam swath bathymetric data (Hogan et al., Submitted.), which was down
sampled to 1 km mesh raster for this study.

2.2 Recovering sub-ice-shelf bathymetry

To recover a gravity-enhanced bathymetry we follow an algorithmic approach, rather than a pure inversion (Hodgson et al.,
2019). We refer to this as the *topographic shift* method, as an initial topographic estimate derived from the gravity data is
125   shifted to match observed topographic tie points. Summarising the method, the initial topographic estimate was calculated
from the free-air anomaly (Fig. 1c, and SFig. 1a) using an iterative forward modelling method (von Frese et al., 1981).
Differences with observed bathymetry and onshore topography were calculated (Fig. 1d, and SFig. 1b), interpolated using a
tensioned spline (Smith and Wessel, 1990), and then subtracted from the initial topographic estimate to provide the final
bathymetric estimate (Fig. 2a). For full detail on the method see supplementary material Section S1. The topographic shift
130   method is conceptually similar to the *gravity shift* method applied along the Greenland coast where the initial free-air gravity
data were shifted to match the variable gravity field from models of known topography prior to inversion for bathymetry (An

et al., 2019). The advantage of both of these techniques is that features in the gravity field due to variations in crustal thickness, sedimentary basins or intrusions are implicitly taken into account, as long as they overlap with the topographic control points. This assumption is most robust for long wavelength features such as variations in crustal thickness, or regional sedimentary

135   basins, where the associated errors will impact multiple topographic control points allowing good control of the resulting error field. The impact of more localised geological features which only partially overlap constraining topographic data will be less well defined and we make the assumption that such errors fall off smoothly away from the control points. Geological features which have no overlap with constraining topographic observations can still introduce artefacts distorting the recovered bathymetry in proportion to their size and density contrast.

140

2.3 Ice shelf draft and cavity thickness

The depth of the ice shelf base, and the thickness of the sub-ice-shelf water filled cavity (Fig. 2b) were calculated assuming the ice shelf is in hydrostatic balance (Griggs and Bamber, 2011). Hydrostatically defined draft is typically a good approximation to radar measured ice thickness (Griggs and Bamber, 2011) and provides seamless coverage of our study area.

145   The input surface elevation data were taken from the REMA digital elevation model (DEM) (Howat et al., 2019) corrected to the GL04c Geoid (Forste et al., 2008). In the study area the REMA DEM is based on satellite observations between 2014 and 2016, and therefore reflects the surface elevation after widespread un-grounding between 1993 and 2014 (Rignot et al., 2014). Ice and water densities were assumed to be 917 and 1027 kg m^{-3}, respectively, and a 16 m firn correction was applied (Griggs and Bamber, 2011). Uncertainties in these assumed values may have an impact on the precise values of ice shelf draft, but are

150   unlikely to significantly distort the calculated pattern of water cavity thickness. Errors in ice shelf draft of up to 80 m in the 10-25 km most proximal to the grounding line may occur due to the rigidity of the ice shelf (Rignot et al., 2011), but in Thwaites glacier this 'bending zone' appears to be narrow (<5 km) (Milillo et al., 2019), which we attribute to the highly fractured nature of the ice shelf in this region.

3 Results

155   Our modelled sub-ice-shelf bathymetry (Fig. 2a) reveals a complex offshore topography from ~250 to >1000 m deep, with a pattern of ridges and troughs of a size and scale consistent with the terrain mapped onshore with radar, and offshore with multi-beam swath bathymetry. All the key bathymetric features we observe are imaged in the free-air gravity data, and are therefore not artefacts of the inversion. Many of the isolated pinning points seaward of Thwaites Glacier and beneath the Crosson Ice Shelf shown by InSAR-derived grounding lines (Rignot et al., 2014) are revealed by our study as being underlain by broader

160   bathymetric highs. In these areas our recovered topography predicts that the ice shelf is grounded, or be within 100 m of grounding (i.e., the water column is calculated to be less than 100 m thick; Fig. 2b). As our inversion did not use any additional

data (swath, seismic or radar) to constrain the elevation at these isolated pinning points within the ice shelves the fact that many appear to be within error of their grounding level provides qualitative support for the reliability of our inversion.

The revealed sub-ice-shelf cavity is >500 m thick in many areas. Adjacent to parts of Thwaites Glacier this deep cavity reaches
165   to within 0-10 km of the grounding line. In contrast the inboard parts of the Dotson and Crosson Ice Shelves formed since 1993 overlie a cavity typically <150m thick (Fig. 2b), and the thick (>450 m) cavity lies more than 10-30 km from the current grounding line.

Profiles of the bathymetry beneath the ice shelves confirm the complex sub-ice-shelf pattern (Fig. 3). Our results show that the tips of both the Eastern Ice Shelf and Thwaites Glacier Tongue are grounded at their seaward ends on a linear but dissected
170   ridge, while a ~1000 m deep sub-ice-shelf cavity is apparent behind the pinning ridge (Figs. 3a and b). Where the grounding line of the Thwaites Glacier Tongue has retreated since 1993 the estimated ice shelf base closely follows the modelled bathymetry (Fig. 3b). Along the narrow channel close to Bear Island a cavity >500 m thick is apparent beneath the Crosson Ice Shelf, but this does not extend into the region where the grounding line has retreated most significantly in the recent decades (Khazendar et al., 2016) (Fig. 3c). Profiles across the Dotson Ice shelf towards Kohler Glacier indicate the grounding line is
175   separated from the main sub-ice-shelf cavity by a sill, which appears to reach within ~200 m of the base of the ice shelf (Figs. 2b and 3d).

4 Discussion

4.1 Quantification of errors

Quantification of the errors associated with gravity inversions is challenging as a combination of intrinsic but quantifiable
180   uncertainties in the gravity data, the inversion assumptions, and the poorly understood variability of sub-surface geology all contribute to the error budget. Errors in the gravity field of ~1.56 mGal defined from crossover analysis directly contribute to ~23m uncertainty in the recovered bathymetry. The modelled rock density of 2670 kg m^{-3} assumes no sediments are present at the sea floor. This is reasonable given the generally rugged morphology observed across many parts of the Amundsen Sea inner shelf (Nitsche et al., 2013;Graham et al., 2009;Larter et al., 2009). However, assuming all bathymetry was carved into
185   lithified sediment the total amplitude of the sub-ice-shelf topography could be underestimated by ~11% (~130 m), assuming a typical sediment density of 2500 kg m^{-3} (Telford et al., 1990). Lower density un-lithified sediment could lead to an even larger underestimates of topographic amplitude, but such material would not be expected to form all of the >1000 m high ridges recovered by our inversion. Other geological factors such as dense gabbroic intrusions, or local sedimentary basins could further distort the recovered bathymetry if they are away from the direct bathymetric observations which would mitigate the
190   impact of such features on the final bathymetric model. Underlying geological factors can, in some cases, be revealed by coincident aeromagnetic data, as in the case of the Brunt Ice Shelf (Jordan and Becker, 2018;Hodgson et al., 2019) and Ross Ice Shelf (Tinto et al., 2019). In our study, tight correlation between high amplitude magnetic and gravity anomalies is only seen beneath the grounded part of Thwaites Glacier (Fig. 3b). Such tight correlation is indicative of a significant geological

feature distorting the gravity signature (Jordan and Becker, 2018), but is not seen on profiles across the offshore regions (Fig.
195   3). This favours a model where underlying geological factors are not dominating the inversion results.

To best quantify the uncertainty in the sub-ice-shelf bathymetric estimate in our study region we utilised the new shipborne
multibeam bathymetric data collected predominantly by a recent ITGC cruise, NBP19-02 (Fig. 1a) (Hogan et al., Submitted.
). The topographic shift method was re-run with this multibeam data excluded from the constraining bathymetric dataset (Fig.
4a). The difference between the results with and without this test dataset (Figs. 4a and b) provides a snap-shot of the errors
200   associated with our recovered bathymetry (Fig. 4c). In this region the mean error is -40 m, with a standard deviation of 100 m.
We take this standard deviation to be representative of the expected error in our modelled bathymetry. The mean error indicates
that the bathymetry constrained by the swath data is deeper than predicted by the gravity inversion alone, and hence that that
there are geological features in this region distorting the recovered bathymetry. It is apparent that the largest errors are
associated with higher frequency topography revealed by the new multibeam data. Such errors resulting from comparison of
205   datasets with fundamentally different resolutions is to be expected, highlighting the need for multibeam bathymetry in regions
where sub-kilometre-scale resolution of bathymetry is required. This is particularly relevant in areas where there the seabed
topography includes high amplitude variations at short wavelengths. In addition, this pattern of errors means that single seismic
observations of cavity depth may not be ideal tie points for gravity inversions in rugged regions such as near Thwaites Glacier.
A single such seismic measurement typically relies on a receiver array ~250 m long (Brisbourne et al., 2014) and hence could
210   image a local high or low, biasing the wider gravity inversion.

4.2 Previous bathymetric estimates

Comparison between our topographic shift method and previous gravity inversions in this region show the broad sub-ice-shelf
features are resolved by all methods, but differences in the detailed results are clear (SFig. 4). The OIB Level 3 data product
(Tinto et al., 2011;Tinto and Bell, 2011) shows the largest discrepancies (SFigs. 4a,d and Figs. 3a,b), with our new inversion
215   showing bathymetry 200 to 300 m shallower at the grounding line. This in part reflects the fact that the OIB bathymetric
estimate was limited to using 2011 and older gravity data. In addition this bathymetric model relied on integrating the results
of a series of 2D forward models, incorporating observed bathymetry and radar-derived topography of grounded ice. These
gravity models did not factor in any regional trends in the gravity field, but rather corrected for a single DC shift at the outboard
end of each profile, and modified the upper crustal density at the inland end of the profile to achieve a good fit. Un-modelled
220   regional trends could, therefore, be a factor distorting the recovered bathymetry.

The Millan et al. (2017) inversion of bathymetry from gravity data shows the same general pattern of sub-ice-shelf bathymetry
as our topographic shift method (SFig. 4b). However, differences are observed, most clearly beneath the inboard parts of the
Dotson Ice Shelf (SFig. 3e). In addition significant undulation in the recovered bathymetry, not associated with any gravity
signal are seen, for example from 100 to 120 km in Figure 3d. Such variability is indicative of artefacts due to the inversion
225   approach. As our topographic shift method is different, and we incorporate additional gravity and bathymetric data, it is not
immediately clear what the source of these discrepancies are. To independently asses the results of Millan et al., (2017) we

calculate a revised bathymetry (SFig. 4c) using the same input data and the gravity shift method previously applied to the Greenland margin (An et al., 2019). The key difference between the An et al., (2019) and Millan et al., (2017) methods is that the newer approach applies a variable rather than single DC shift to the gravity prior to inverting for the bathymetry, but in other respects the methods closely match. The residuals between the Millan et al., 2017 result and the gravity shift method (SFig. 4f) shows a similar pattern to the residuals between the Millan et al., 2017 result and our topographic shift method (SFig. 4e). This indicates that the use of a single DC shift was a significant issue in the older inversion (Millan et al., 2017) which may have led to an over-estimate of the depth of some near-shore features. Comparing the gravity shift and topographic shift results reveals that differences of over 250 m are still present (SFig. 4g). We suggest that these remaining differences reflect the additional multibeam bathymetric and gravity data used in our topographic shift result, the different bed topography onshore (OIB flights here vs. mass conservation in Millan et al., 2017) and exclusion of sub-ice-shelf pinning points from the topographic shift result. This highlights the need for caution when using -gravity-derived bathymetry and the value of high resolution gravity data with tight line spacing such as the ITGC dataset, together with additional well-constrained and well distributed observational tie points beneath the ice shelves.

4.3 Implications for the Amundsen Sea ice shelves

4.3.1 Pathways for water

The results of our new bathymetric estimates have significant implications for how we understand the pattern of cryospheric changes occurring in the Thwaites, Dotson and Crosson areas. Our primary observation confirms that the ice front in the centre of Thwaites Glacier is directly and easily accessible to mCDW through a channel over 800 m deep beneath the Thwaites Eastern Ice Shelf and Thwaites Glacier Tongue (Millan et al., 2017;Tinto and Bell, 2011) (Fig. 2a). This trough is separated from an adjacent >1000 m deep trough by a ridge that is in places <150 m deep where the Eastern Ice Shelf and Thwaites Glacier Tongue grounded. However, 700 to 800 m deep channels cut the ridge, linking the two troughs, and potentially facilitating lateral circulation beneath the ice shelves. As mCDW is warmer than the typical shelf water, its circulation can contribute to ice shelf and ice sheet grounding line melting (Jenkins et al., 2010).

The Crosson Ice Shelf is underlain by bathymetry 300 to 500 m deep, shallower than the typical core of the mCDW (Assmann et al., 2013). A 700 – 1000 m deep channel is present flanking Bear Island (Figs. 2b and 3c), but its width of just 10 km suggests that flux of mCDW may be less via this route. However, in some years the upper boundary of the mCDW can sit around 400-600 m deep (Dutrieux et al., 2014;Jenkins et al., 2018), shallower than much of the bathymetry beneath the Crosson Ice Shelf, meaning mCDW could still access the inner Crosson cavity. The final ~30 km to the most recent grounding line of Smith Glacier are characterised by a cavity typically 100-200 m thick, which could limit the supply of mCDW water to the grounding line. The Dotson Ice Shelf is underlain by a broad cavity >800 m deep and is separated from the currently rapidly-changing grounding line of the western branch of the Kohler Glacier by a sill 700-800 m deep (Fig. 3d). This sill may partially

shield this grounding line from oceanographically-driven change, as the bulk of the inflowing mCDW is mapped at a depth of ~800 m at the Dotson ice shelf margin (Miles et al., 2016).

4.3.2 Two ice shelf populations

A second key observation is that the ice shelves in areas which ungrounded since measurement of the 1993 grounding line are all underlain by relatively thin cavities (Fig. 2b). Such thin cavity geometry in newly un-grounded regions is predicted by some fully coupled, ice-ocean numerical models of ice sheet retreat (Seroussi et al., 2017). These newly formed regions of floating ice (Fig. 1d) appear to be distinct from the wider, more established, ice shelf system which is underlain by both thick and thin cavities. This pattern is not simply a result of distance from the grounding line, as in places where the ice shelf has not retreated thick cavities are seen at the grounding line, for example west of Thwaites Glacier tongue, and East of Pope Glacier (Fig. 2b). To consider the different ice shelf systems in more detail we plotted hydrostatic ice shelf draft against our recovered bathymetry (Fig. 5). The older ice shelves, outboard from the 1993 grounding line, show limited correlation with the underlying bathymetry (Fig. 5a). This is expected given the shelves float passively over the underlying topography. Regionally the main control on the draft of these ice shelves is likely the depth of top of the mCDW, which would drive enhanced basal melt. The fact that few of the older ice shelves have depths greater than 500 m would be consistent with this hypothesis, as mCDW at depths of 400 to 800 m is observed in oceanographic transects at the ice shelf edge (Miles et al., 2016;Dutrieux et al., 2014;Jenkins et al., 2018;Jacobs et al., 1996). The slight positive correlation between depth and thinner ice shelves (Fig. 5a) may reflect shallow bathymetry forcing mCDW to shallower levels.

The draft in newly established ice shelf areas shows an almost 1:1 relationship with the underlying bathymetry (Fig. 5b). The difference between the bed elevation and ice shelf draft suggests that these newly formed cavities are on average 112 m thick, with >95% being <~400 m thick. The rapid grounding line retreat which led to the formation of the post-1993 ice shelf sectors has been regarded as a harbinger of catastrophic collapse of the Amundsen Sea sector of the West Antarctic Ice Sheet through geometric marine ice sheet instability, unconstrained by inland pinning points (Rignot et al., 2014). It has been suggested that basal melting driven by ingress of warmer mCDW could be a key factor facilitating this process (Milillo et al., 2019;Pritchard et al., 2012). Our results indicate there is generally a close relationship between bed elevation, cavity thickness and ice shelf draft in the newly un-grounded regions. We consider two end-member conceptual mechanisms which could have driven the rapid grounding line retreat and development of the observed cavity geometry; ice flow acceleration coupled with geometric spreading, or enhanced grounding line melt (Fig. 6).

In the case of geometric spreading (Fig. 6a), accelerating ice flow means the ice sheet thins. As the ice sheet reaches its hydrostatic limit it un-grounds. When this occurs on a retrograde bed, as is the case for the majority of our study region (Fig. 3), the non-linear dependence of the ice flow speed across the grounding line on the ice thickness facilitates further acceleration and un-grounding (Schoof, 2007). The process of acceleration could be initiated by un-grounding of a buttressing ice shelf from critical pinning points, or ice shelf thinning due to enhanced basal melting. This mechanism can explain rapid grounding line retreat, without the need for sustained penetration of warm ocean water through a narrow sub-ice-shelf cavity. However,

in this scenario there is no clear mechanism for maintaining a cavity with a relatively uniform thickness following the underlying topography once the system is un-grounded.

Where grounding line retreat is driven by melting, very high melt rates are likely focused at the grounding line (Fig. 6b) (Lilien et al., 2019). This could reflect the first interaction between warm saline mCDW, the front of the grounded ice sheet and fresh

295 subglacial melt water if any exists (Fig. 6b). In our conceptual model enhanced basal melting remains focused at the grounding line until the ice thins enough to un-ground. The enhanced melting zone moves further inboard with the grounding line, and negative feedbacks such as cooling and dilution of the mCDW, and the higher pressure melting temperature at shallower depths inhibits further significant erosion of the cavity. Enhanced melting of up to 200 m per year has been calculated from satellite observations and OIB radar profiles over the new Thwaites Glacier ice shelves (Milillo et al., 2019), and rates of 50-70 m a^{-1}

300 have been observed close to the grounding line of Smith Glacier (Khazendar et al., 2016). However, our data indicate that the highest of these melt rates must be spatially limited, as the newly formed cavity thickness typically does not exceed ~400 m, i.e. approximately two years of the most elevated melt rates, and 8 years at the lower end of the enhanced melt rates. We propose that the fast flowing ice is advected across the region of most enhanced melting, limiting thinning and preserving the cavity.

305 In the Smith Glacier region comparison of 2016 OIB radar with earlier radar data allows reconstruction of the spatial distribution of the most recent ice shelf thinning (Fig. 7). These direct observations confirm, as predicted from our cavity thickness estimate, that across much of the new ice shelf, thinning rates are relatively low, hence a relatively thin cavity can be maintained. However, they also reveal that the enhanced thinning rates of 50-70 m a^{-1} beneath the inner shelf noted for the period 2002 to 2009 (Khazendar et al., 2016) have continued into the period 2009-2016. These high rates appear to be restricted

310 to the area where the base of the ice shelf is >1200 m deep. One possibility is that mCDW is penetrating to the grounding line, but it is not clear to what extent this water would have been mixed and diluted during its passage through the <400 m thick sub-ice shelf cavity. Also, the ice-shelf marginal weakening and consequent ice acceleration likely contributed to the observed fast grounding-line retreat and thinning at the grounding line (Lilien et al., 2019).

We do not consider the geometric or basal melt mechanisms outlined above to be mutually exclusive. However, the consistent

315 presence of broad but vertically thin subglacial cavities appears to be most challenging for a purely melt driven model, as access by warm water to the grounding line would be hampered by the thin cavity (Schoof, 2007). This physical limitation is supported by models for Pine Island Glacier margin, which indicated that cavities <200 m thick slowed the ingress of warm bottom water over topographic ridges (De Rydt et al., 2014). More complex fully coupled ocean-ice models also show the development of thin cavities and indicate that the associated weak circulation acts to slow grounding line retreat relative to

320 that predicted by an un-coupled model (Seroussi et al., 2017).

The contrast in cavity geometry and relationship to the underlying bathymetry of the pre and post 1993 ice shelf regions suggests that the recently un-grounded regions may not yet be in equilibrium with the wider glaciological and oceanic system. As such, they may play a significant, but as yet poorly understood role in controlling the future evolution of the ice sheet marginal system. The thin cavities in particular may act to slow future changes. Firstly, they place a fundamental limit onto

325   the amount of warm water which can flux beneath the glacier, and may also facilitate the tidally-driven turbulent flow mixing of water masses before they can reach the grounding line (Holland, 2008). In addition, the thin cavities which we observe are particularly sensitive to re-grounding on retrograde slopes, a negative feedback which would act to temporally re-stabilise a retreating ice sheet. This process of grounding line re-advance appears to have occurred in the Western Kohler Glacier (Fig. 1a), where the 2014 grounding line lies downstream of the 2012 grounding line (Rignot et al., 2014). Our observations of
330   consistent thin cavities in newly un-grounded regions supports the results of coupled ocean-ice models confirming the necessity of such detailed modelling for predicting the evolution of the Thwaites Glacier system (Seroussi et al., 2017).

5. Conclusions

Airborne gravity provides a good first order estimate of sub-ice-shelf bathymetry. Despite the relatively high uncertainty (~100 m standard deviation) comparisons with different gravity inversion techniques, and new observational bathymetric data,
335   indicate that the pattern of sub-ice-shelf bathymetry is well resolved.

Thwaites Glacier is connected to the deep ocean by a major trough >800 m deep and 20 km wide. In contrast the grounding lines of the of Dotson and Crosson ice shelves are accessible through relatively narrow channels and thin sub shelf cavities. In the Thwaites, Dotson and Crosson region, areas of ice shelf which developed before and after 1993 form distinct populations. The most recently un-grounded areas are underlain by thin cavities (average 112 m) where the ice shelf base closely tracks the
340   underlying bed topography. We propose that these systems represent a transient phase of ice margin development, which may act to slow future changes, which is indicated but not fully captured in present models.

Data availability

ITGC airborne geophysical data is available from the UK Polar Data Centre upon publication of this paper. Input topography, gravity grids and model bathymetry will also be available from the same source. Other data is from sources cited in the text.

345   ### Author Contributions

All authors contributed to the discussion and production of the final manuscript.
Additional specific contributions include:
Tom Jordan – Gravity data processing, topographic shift bathymetric inversion and primary manuscript preparation.
David Porter – Airborne gravity and magnetic data collection.
350   Kirsty Tinto – Discussion of bathymetry inversion techniques.
Romain Millan – Discussion of gravity inversion and preparation of gravity shift bathymetric model.
Atsuhiro Muto - Discussion of gravity inversion and implications of ice sheet cavity findings.

Kelly Hogan – Preparation of multibeam bathymetry.

Rob Larter – Provision of ship-borne gravity and swath data.

355 Ali Graham – processing and preparation of swath bathymetry data on NBP19-02.

John Paden – developed the airborne radar system, processed the data, and picked the ice sheet bed.

Competing Interests

None

Acknowledgements

360 This work is a British Antarctic Survey (BAS) National Capability contribution to the International Thwaites Glacier
Collaboration (ITGC), with additional support from the BAS Geology and Geophysics Team (TJ). Additional support for this
work is from Lamont-Doherty Earth Observatory NSF grant number NSF1842064 (DP, KT), and the THOR (KH, RL, AG,
and Cruise NBP19 02) and TARSAN (AM) projects, components of the International Thwaites Glacier Collaboration (ITGC).
Support from National Science Foundation (NSF: Grant NSFPLR-NERC-1738942 for THOR, NSFPLR-NERC-1738992 for

365 TARSAN) and Natural Environment Research Council (NERC: Grant NE/S006664/1 for THOR, NE/S006419/1 for
TARSAN).

References

Abulaitijiang, A., Andersen, O. B., and Sandwell, D.: Improved Arctic Ocean Bathymetry Derived From DTU17 Gravity Model, Earth and Space Science, 6, 1336-1347, 10.1029/2018EA000502, 2019.

370 An, L., Rignot, E., Millan, R., Tinto, K., and Willis, J.: Bathymetry of Northwest Greenland Using "Ocean Melting Greenland" (OMG) High-Resolution Airborne Gravity and Other Data, Remote Sensing, 11, https://doi.org/10.3390/rs11020131 2019.

Assmann, K. M., Jenkins, A., Shoosmith, D. R., Walker, D. P., Jacobs, S. S., and Nicholls, K. W.: Variability of Circumpolar Deep Water transport onto the Amundsen Sea Continental shelf through a shelf break trough, Journal of Geophysical Research: Oceans, 118, 6603-6620, 10.1002/2013JC008871, 2013.

375 Becker, D., Nielsen, J. E., Ayres-Sampaio, D., Forsberg, R., Becker, M., and Bastos, L.: Drift reduction in strapdown airborne gravimetry using a simple thermal correction, Journal of Geodesy, 89, 1133-1144, 2015.

Brisbourne, A. M., Smith, A. M., King, E. C., Nicholls, K. W., Holland, P. R., and Makinson, K.: Seabed topography beneath Larsen C Ice Shelf from seismic soundings, The Cryosphere, 8, 1-13, 10.5194/tc-8-1-2014, 2014.

Cochran, J. R., and Bell, R. E.: Inversion of IceBridge gravity data for continental shelf bathymetry beneath the Larsen Ice Shelf, Antarctica,

380 Journal of Glaciology, 58, 540-552, doi: 510.3189/2012JoG3111J3033, 2012.

Cochran, J. R., Jacobs, S. S., Tinto, K. J., and Bell, R. E.: Bathymetric and oceanic controls on Abbot Ice Shelf thickness and stability, The Cryosphere, 8, 877-889, 10.5194/tc-8-877-2014, 2014.

Davies, D., Bingham, R. G., Graham, A. G. C., Spagnolo, M., Dutrieux, P., Vaughan, D. G., Jenkins, A., and Nitsche, F. O.: High-resolution sub-ice-shelf seafloor records of twentieth century ungrounding and retreat of Pine Island Glacier, West Antarctica Journal of Geophysical

385 Research, 122, 1698-1714. https://doi.org/1610.1002/2017JF004311, 2017.

De Rydt, J., Holland, P. R., Dutrieux, P., and Jenkins, A.: Geometric and oceanographic controls on melting beneath Pine Island Glacier, Journal of Geophysical Research: Oceans, 119, 2420-2438, 10.1002/2013JC009513, 2014.

Dutrieux, P., De Rydt, J., Jenkins, A., Holland, P. R., Ha, H. K., Lee, S. H., Steig, E. J., Ding, Q., Abrahamsen, E. P., and Schröder, M.: Strong Sensitivity of Pine Island Ice-Shelf Melting to Climatic Variability, Science, 343, 174, 10.1126/science.1244341, 2014.

390   Forste, C., Schmidt, R., Stubenvoll, R., Flechtner, F., Meyer, U., Konig, R., Neumayer, H., Biancale, R., Lemoine, J. M., Bruinsma, S., Loyer, S., Barthelmes, F., and Esselborn, S.: The Geo-ForschungsZentrum Potsdam/Groupe de Recherche de Geodesie Spatiale satellite-only and combined gravity field models:EIGEN-GL04S1 and EIGEN-GL04C, J. Geodesy, 82, 331–346,doi:310.1007/s00190-00007-00183-00198, 02008, 2008.

      Fretwell, P., Pritchard, H. D., Vaughan, D. G., Bamber, J., Barrand, N., Bell, R., Bianchi, C., Bingham, R., Blankenship, D., Casassa, G.,
395   Callens, D., Conway, H., Cook, A. J., Corr, H. F. J., Damaske, D., Damm, V., Ferraccioli, F., Forsberg, R., Fujita, S., Gogineni, P., Griggs, J. A., Hindmarsh, R., Holmlund, P., Holt, J. W., Jacobel, R. W., Jenkins, A., Jokat, W., Jordan, T. A., King, E. C., Kohler, J., Krabill, W., Riger-Kusk, R., Langley, K. A., Leitchenkov, G., Leuschen, C., Luyendyk, B. P., Matsuoka, K., Nogi, Y., Nost, O. A., Popov, S., Rignot, E., Rippin, D. M., Riviera, A., Roberts, J., Ross, N., Siegert, M. J., Smith, A. M., Steinhage, D., Studinger, M., Sun, B., Tinto, B. K., Welch, B. C., Young, D. A., Xiangbin, C., and Zirizzotti, A.: Bedmap2: improved ice bed, surface and thickness datasets for Antarctica, The
400   Cryosphere, 7, 2013.

      Gardner, A. S., Moholdt, G., Scambos, T., Fahnstock, M., Ligtenberg, S., van den Broeke, M., and Nilsson, J.: Increased West Antarctic and unchanged East Antarctic ice discharge over the last 7 years, The Cryosphere, 12, 521-547, 10.5194/tc-12-521-2018, 2018.

      Golynsky, A. V., Ferraccioli, F., Hong, J. K., Golynsky, D. A., Frese, R. R. B., Young, D. A., Blankenship, D. D., Holt, J. W., Ivanov, S. V., Kiselev, A. V., Masolov, V. N., Eagles, G., Gohl, K., Jokat, W., Damaske, D., Finn, C., Aitken, A., Bell, R. E., Armadillo, E., Jordan,
405   T. A., Greenbaum, J. S., Bozzo, E., Caneva, G., Forsberg, R., Ghidella, M., Galindo-Zaldivar, J., Bohoyo, F., Martos, Y. M., Nogi, Y., Quartini, E., Kim, H. R., and Roberts, J. L.: New Magnetic Anomaly Map of the Antarctic, Geophysical Research Letters, 45, 6437-6449, doi:10.1029/2018GL078153, 2018.

      Gómez-Ortiz, D., and Agarwal, B. N. P.: 3DINVER.M: a MATLAB program to invert the gravity anomaly over a 3D horizontal density interface by Parker–Oldenburg's algorithm, Computers & Geosciences, 31, 513-520, https://doi.org/10.1016/j.cageo.2004.11.004, 2005.
410   Graham, A. G. C., Larter, R. D., Gohl, K., Hillenbrand, C.-D., Smith, J. A., and Kuhn, G.: Bedform signature of a West Antarctic palaeo-ice stream reveals a multi-temporal record of flow and substrate control, Quaternary Science Reviews, 28, 2774-2793, https://doi.org/10.1016/j.quascirev.2009.07.003, 2009.

      Griggs, J. A., and Bamber, J. L.: Antarctic ice-shelf thickness from satellite radar altimetry, Journal of Glaciology, 57, 485-498, 10.3189/002214311796905659, 2011.
415   Hodgson, D. A., Jordan, T. A., De Rydt, J., Fretwell, P. T., Seddon, S. A., Becker, D., Hogan, K. A., Smith, A. M., and Vaughan, D. G.: Past and future dynamics of the Brunt Ice Shelf from seabed bathymetry and ice shelf geometry, The Cryosphere, 13, 545-556, 10.5194/tc-13-545-2019, 2019.

      Hogan, K., Larter, R., Graham, A. G. C., Arthern, R., Kirkham, Totten Minzoni, R., Jordan, T. A., Clark, Fitzgerald, Anderson, Hillenbrand, Nitsche, Simkins, Smith, Gohl, Hong, and Wellner: Revealing the former bed of Thwaites Glacier using high-resolution bathymetric data,
420   The Cryosphere, Submitted. .

      Holland, P. R.: A model of tidally dominated ocean processes near ice shelf grounding lines, Journal of Geophysical Research: Oceans, 113, 10.1029/2007JC004576, 2008.

      Holt, J. W., Blankenship, D. D., Morse, D. L., Young, D. A., Peters, M. E., Kempf, S. D., Richter, T. G., Vaughan, A. P. M., and Corr, H.: New Boundary Conditions for the West Antarctic Ice Sheet: Subglacial Topography of the Thwaites and Smith Glacier Catchments.,
425   Geophysical Research Letters, 33, doi:10.1029/2005GL025561, 2006.

      Howat, I. M., Porter, C., Smith, B. E., Noh, M. J., and Morin, P.: The Reference Elevation Model of Antarctica, The Cryosphere, 13, 665-674, 10.5194/tc-13-665-2019, 2019.

      Jacobs, S. S., Hellmer, H. H., and Jenkins, A.: Antarctic Ice Sheet melting in the southeast Pacific, Geophysical Research Letters, 23, 957-960, 10.1029/96GL00723, 1996.
430   Jacobs, S. S., Jenkins, A., Giulivi, C. F., and Dutrieux, P.: Stronger ocean circulation and increased melting under Pine Island Glacier ice shelf., Nature Geosci, 4, 519–523, 2011.

      Jenkins, A., Dutrieux, P., Jacobs, S. S., McPhail, S. D., Perrett, J. R., Webb, A. T., and White, D.: Observations beneath Pine Island Glacier in West Antarctica and implications for its retreat, Nature Geoscience, 3, 468 - 472. doi:410.1038/ngeo1890, 2010.

      Jenkins, A., Shoosmith, D., Dutrieux, P., Jacobs, S., Kim, T. W., Lee, S. H., Ha, H. K., and Stammerjohn, S.: West Antarctic Ice Sheet
435   retreat in the Amundsen Sea driven by decadal oceanic variability, Nature Geoscience, 11, 733-738, 10.1038/s41561-018-0207-4, 2018.

      Jordan, T. A., and Becker, D.: Investigating the distribution of magmatism at the onset of Gondwana breakup with novel strapdown gravity and aeromagnetic data, Physics of the Earth and Planetary Interiors, 282, 77-88, https://doi.org/10.1016/j.pepi.2018.1007.1007, 2018.

      Khazendar, A., Rignot, E., Schroeder, D. M., Seroussi, H., Schodlok, M. P., Scheuchl, B., Mouginot, J., Sutterley, T. C., and Velicogna, I.: Rapid submarine ice melting in the grounding zones of ice shelves in West Antarctica, Nature Communications, 7, 13243,
440   10.1038/ncomms13243 https://www.nature.com/articles/ncomms13243#supplementary-information, 2016.

      Larter, R. D., Graham, A. G. C., Gohl, K., Kuhn, G., Hillenbrand, C.-D., Smith, J. A., Deen, T. J., Livermore, R. A., and Schenke, H.-W.: Subglacial bedforms reveal complex basal regime in a zone of paleo–ice stream convergence, Amundsen Sea embayment, West Antarctica, Geology, 37, 411-414, 10.1130/G25505A.1, 2009.

445 Lilien, D. A., Joughin, I., Smith, B., and Gourmelen, N.: Melt at grounding line controls observed and future retreat of Smith, Pope, and Kohler glaciers, The Cryosphere, 13, 2817-2834, 10.5194/tc-13-2817-2019, 2019.

Miles, T., Lee, S. H., Wåhlin, A., Ha, H. K., Kim, T. W., Assmann, K. M., and Schofield, O.: Glider observations of the Dotson Ice Shelf outflow, Deep Sea Research Part II: Topical Studies in Oceanography, 123, 16-29, https://doi.org/10.1016/j.dsr2.2015.08.008, 2016.

Milillo, P., Rignot, E., Rizzoli, P., Scheuchl, B., Mouginot, J., Bueso-Bello, J., and Prats-Iraola, P.: Heterogeneous retreat and ice melt of
450 Thwaites Glacier, West Antarctica, Science Advances, 5, eaau3433, 10.1126/sciadv.aau3433, 2019.

Millan, R., Rignot, E., Bernier, V., Morlighem, M., and Dutrieux, P.: Bathymetry of the Amundsen Sea Embayment sector of West Antarctica from Operation IceBridge gravity and other data, Geophysical Research Letters, 44, 1360-1368, 10.1002/2016GL072071, 2017.

Muto, A., Peters, L. E., Gohl, K., Sasgen, I., Alley, R. B., Anandakrishnan, S., and Riverman, K. L.: Subglacial bathymetry and sediment distribution beneath Pine Island Glacier ice shelf modeled using aerogravity and in situ geophysical data: New results, Earth and Planetary
455 Science Letters, 433, 63-75, http://dx.doi.org/10.1016/j.epsl.2015.10.037, 2016.

Nitsche, F. O., Gohl, K., Larter, R. D., Hillenbrand, C. D., Kuhn, G., Smith, J. A., Jacobs, S., Anderson, J. B., and Jakobsson, M.: Paleo ice flow and subglacial meltwater dynamics in Pine Island Bay, West Antarctica, The Cryosphere, 7, 249-262, 10.5194/tc-7-249-2013, 2013.

Pail, R., Goiginger, H., Mayrhofer, R., Schuh, W. D., Brockmann, J. M., Krasbutter, I., Höck, E., and Fecher, T.: GOCE gravity field model derived from orbit and gradiometery data applying the time-wise method, ESA Living Planet Symposium, Bergen, Norway, 2010,
460 Pritchard, H. D., Ligtenberg, S. R. M., Fricker, H. A., Vaughan, D. G., van den Broeke, M. R., and Padman, L.: Antarctic ice-sheet loss driven by basal melting of ice shelves, Nature, 484, 502-505, 10.1038/nature10968, 2012.

Rignot, E., Mouginot, J., and Scheuchl, B.: Antarctic grounding line mapping from differential satellite radar interferometry, Geophysical Research Letters, 38, 10.1029/2011GL047109, 2011.

Rignot, E., Mouginot, J., Morlighem, M., Seroussi, H., and Scheuchl, B.: Widespread, rapid grounding line retreat of Pine Island, Thwaites,
465 Smith, and Kohler glaciers,West Antarctica, from 1992 to 2011, Geophysical Research Letters, 41, 3502-3409, DOI: 3510.1002/2014GL060140, 2014.

Rosier, S. H. R., Hofstede, C., Brisbourne, A. M., Hattermann, T., Nicholls, K. W., Davis, P. E. D., Anker, P. G. D., Hillenbrand, C.-D., Smith, A. M., and Corr, H. F. J.: A New Bathymetry for the Southeastern Filchner-Ronne Ice Shelf: Implications for Modern Oceanographic Processes and Glacial History, Journal of Geophysical Research: Oceans, 123, 4610-4623, doi:10.1029/2018JC013982, 2018.

470 Roy, L., Sen, M. K., Blankenship, D. D., Stoffa, P. L., and Richter, T. G.: Inversion and uncertainty estimation of gravity data using simulated annealing: An application over Lake Vostok, East Antarctica, Geophysics, 70, J1-J12, 10.1190/1.1852777, 2005.

Scambos, T. A., Bohlander, J. A., Shuman, C. A., and Skvarca, P.: Glacier acceleration and thinning after ice shelf collapse in the Larsen B embayment, Antarctica, Geophysical Research Letters, 31, doi:10.1029/2004GL020670, 2004.

Scambos, T. A., Bell, R. E., Alley, R. B., Anandakrishnan, S., Bromwich, D. H., Brunt, K., Christianson, K., Creyts, T., Das, S. B., DeConto,
475 R., Dutrieux, P., Fricker, H. A., Holland, D., MacGregor, J., Medley, B., Nicolas, J. P., Pollard, D., Siegfried, M. R., Smith, A. M., Steig, E. J., Trusel, L. D., Vaughan, D. G., and Yager, P. L.: How much, how fast?: A science review and outlook for research on the instability of Antarctica's Thwaites Glacier in the 21st century, Global and Planetary Change, 153, 16-34, https://doi.org/10.1016/j.gloplacha.2017.04.008, 2017.

Schoof, C.: Ice sheet grounding line dynamics: steady states, stability and hysteresis, Journal of Geophysical Research, 112, F03S28,
480 doi:10.1029/2006JF000664, 2007.

Seroussi, H., Nakayama, Y., Larour, E., Menemenlis, D., Morlighem, M., Rignot, E., and Khazendar, A.: Continued retreat of Thwaites Glacier, West Antarctica, controlled by bed topography and ocean circulation, Geophysical Research Letters, 44, 6191-6199, 10.1002/2017GL072910, 2017.

Smith, W. H. F., and Wessel, P.: Gridding with continuous curvature splines in tension, Geophysics, 55, 293-305, 1990.

485 Smith, W. H. F., and Sandwell, D. T.: Bathymetric prediction from dense satellite altimetry and sparse shipboard bathymetry, Journal of Geophysical Research: Solid Earth, 99, 21803-21824, 10.1029/94JB00988, 1994.

Telford, W. M., Geldart, L. P., and Sheriff, R. E.: Applied Geophysics, 2nd ed., Cambridge University Press, Cambridge, 1990.

Tinto, K. J., and Bell, R. E.: Progressive unpinning of Thwaites Glacier from newly identified offshore ridge: Constraints from aerogravity, Geophysical Research Letters, 38, DOI: 10.1029/2011GL049026, 2011.

490 Tinto, K. J., Padman, L., Siddoway, C. S., Springer, S. R., Fricker, H. A., Das, I., Caratori Tontini, F., Porter, D. F., Frearson, N. P., Howard, S. L., Siegfried, M. R., Mosbeux, C., Becker, M. K., Bertinato, C., Boghosian, A., Brady, N., Burton, B. L., Chu, W., Cordero, S. I., Dhakal, T., Dong, L., Gustafson, C. D., Keeshin, S., Locke, C., Lockett, A., O'Brien, G., Spergel, J. J., Starke, S. E., Tankersley, M., Wearing, M. G., and Bell, R. E.: Ross Ice Shelf response to climate driven by the tectonic imprint on seafloor bathymetry, Nature Geoscience, 12, 441-449, 10.1038/s41561-019-0370-2, 2019.

495 von Frese, R. R. B., Hinze, W. J., Braile, L. W., and Luca, A. J.: Spherical earth gravity and magnetic anomaly modeling by Gauss- Legendre quadrature integration, Journal of Geophysics, 49, 234-242, 1981.

Weertman, J.: Stability of the junction of an ice sheet and an ice shelf, Journal of Glaciology, 13, 3-11, 1974.

Wei, M., and Schwarz, K. P.: Flight test results from a strapdown airborne gravity system, Journal of Geodesy, 72, 323-332, 1998.

500
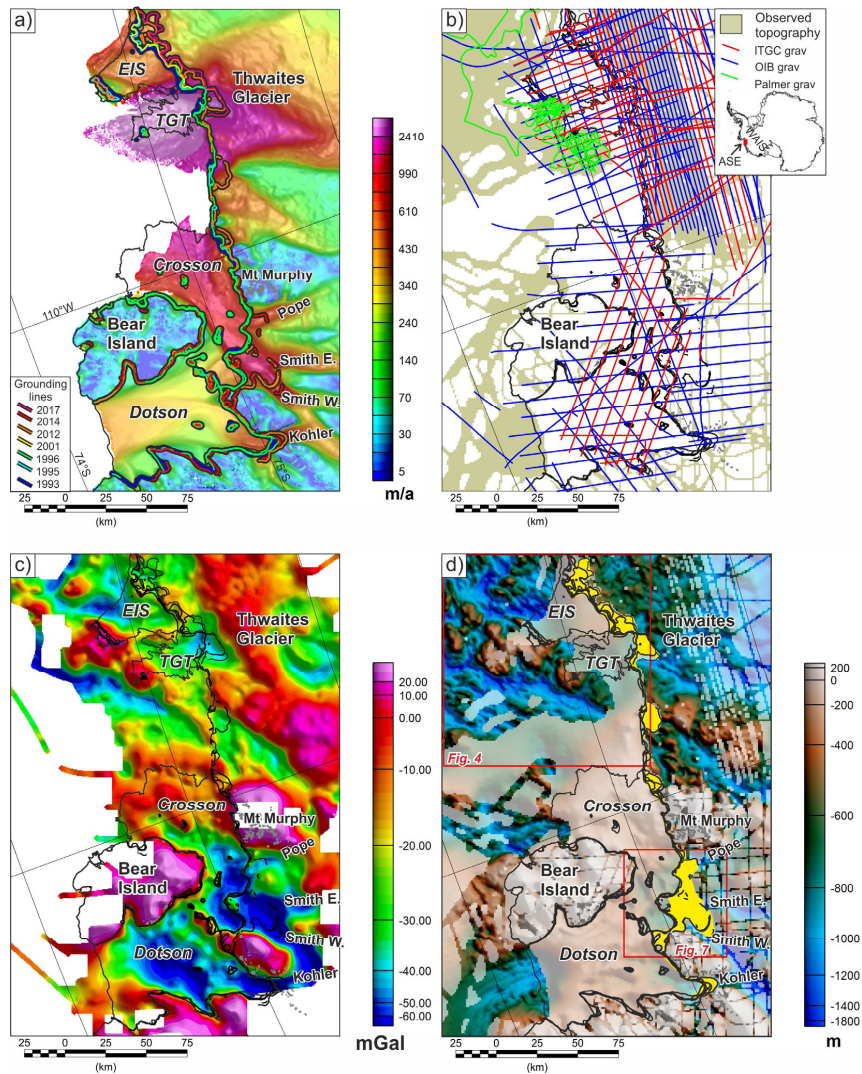
Figure 1: Regional setting and input data. a) Ice velocity (Rignot et al., 2017) with InSAR grounding lines in colour (Rignot et al., 2014;Milillo et al., 2019). Grey lines rock exposures. Thwaites Glacier Tongue (TGT), Eastern ice Shelf (EIS). b) Line gravity data coverage, regions of known topography and inset showing Antarctic context. c) Integrated free air gravity anomaly grid. d) Direct

505 topographic observations (strong colours), onshore from Operation Ice Bridge (OIB) (Paden et al., 2010, updated 2018) and ITGC, and offshore from ship-borne swath coverage (Hogan et al. submit.). Pale colours show BEDMAP2 DEM (Fretwell et al., 2013). Yellow areas highlight post 1993 ice shelves. Red boxes locate figures 4 and 7.
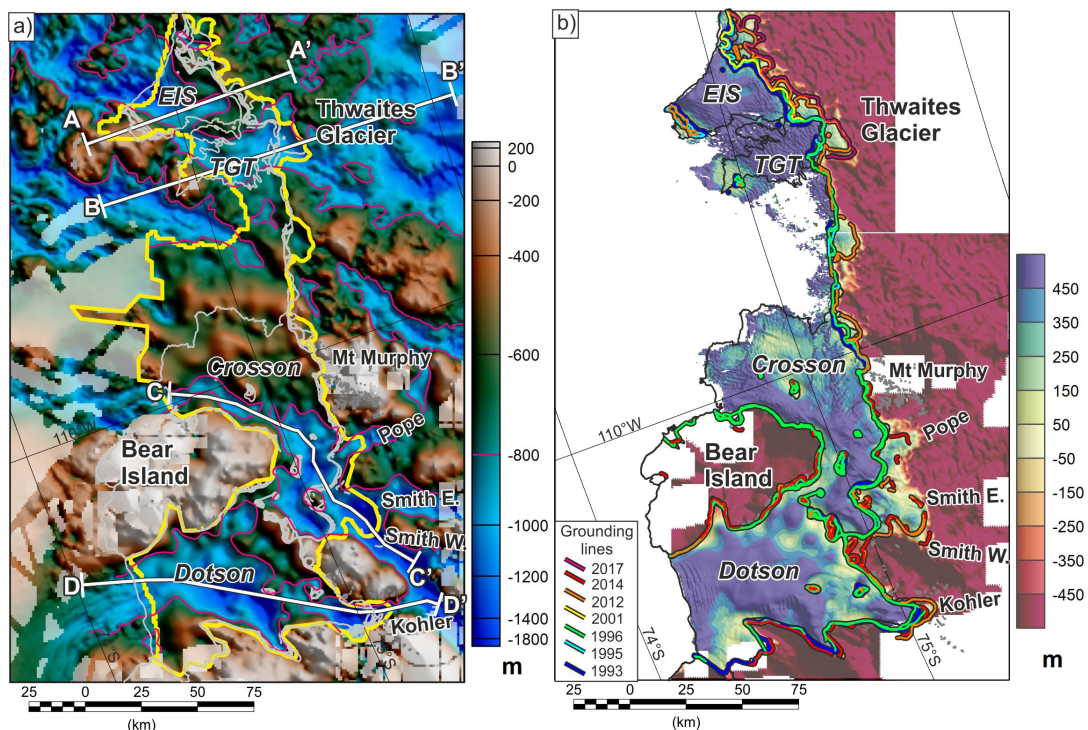
510 **Figure 2: New bathymetry and cavity maps. a) Final topography from terrain shift method. White lines A-D mark profiles in Fig. 3. Yellow outline encloses region constrained by gravity data. Pink line shows -800m depth contour. Light grey lines mark grounding lines and ice shelf edge. b) Sub-ice-shelf water column thickness based on the REMA DEM and an assumption of hydrostatic equilibrium. Regions where the ice sheet is predicted to be grounded show negative cavity thickness.**
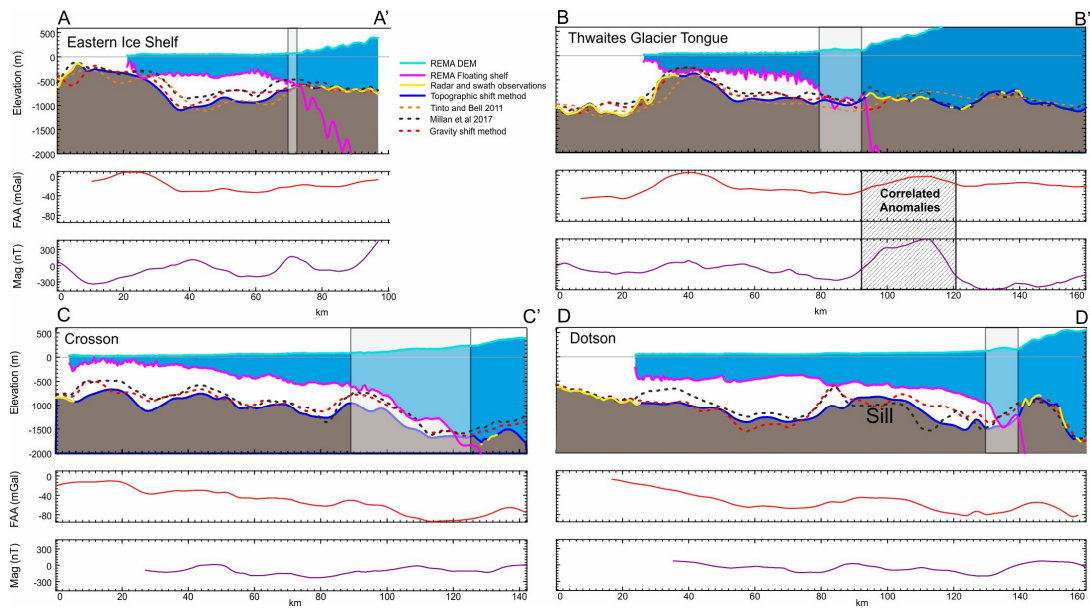
Figure 3: Profiles across ice shelves. Upper panel shows ice surface from REMA DEM (Howat et al., 2019) and base of ice shelf calculated assuming hydrostatic equilibrium, together with gravity-derived bathymetric estimates. Second panel shows input free-air gravity anomaly. Third panel shows magnetic anomalies derived from ITGC survey data (REF data doi) and ADMAP2 (Golynsky et al., 2018). a) Thwaites Eastern Ice Shelf. b) Thwites Glacier Tongue. c) Crosson Ice Shelf. d) Dotson Ice Shelf. Note thin cavity in regions of ice sheet grounding line retreat since 1993 (grey boxes).
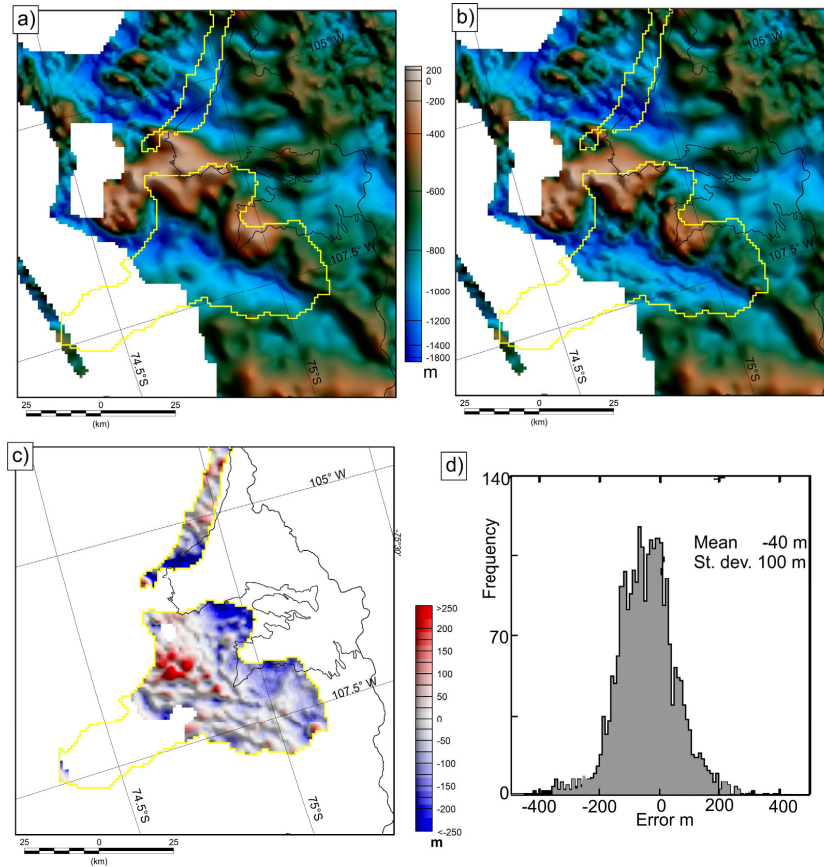
Figure 4: Error estimates. a) Bathymetric estimate excluding bathymetric data from cruises NBP19-02 and JR294 (yellow outlines). b) Bathymetry including new multibeam data (as in Fig. 2a). c) Discrepancy in areas of additional data. d) Histogram of errors in areas of new multibeam constraint.
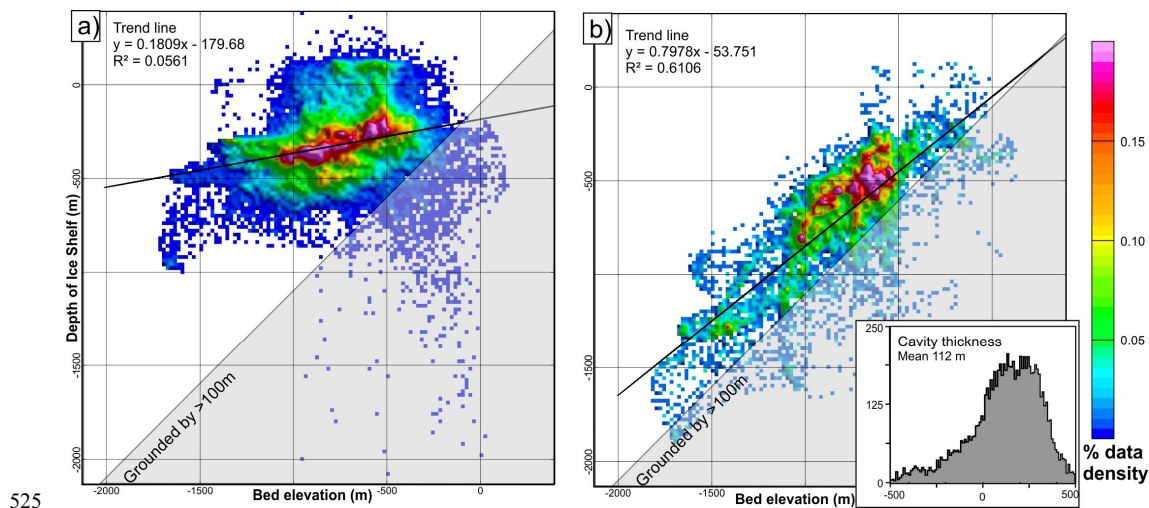
525

Figure 5: Data density plot of hydrostatic ice shelf draft against sub-shelf bathymetry. Trend lines show best linear fit through data point cloud. a) Plot for ice shelves outboard of the 1993 grounding line. b) Plot for ice shelves formed by grounding line retreat since 1993, with inset showing histogram cavity thickness beneath the areas of newly developed ice shelf. Note data where ice shelf depth is >0 m results from regions where the ice shelf surface elevation is less than the firn correction. Points which plot below the 1:1 line are theoretically grounded. However, errors in the gravity derived topography with a standard deviation of ~100 m are noted (Fig. 4d), hence some areas which appear shallowly grounded may in fact be floating. In addition uncertainties in grounding-line position and real pinning points within the areas designated as ice shelves contribute to the observed scatter of anomalous points.

530

535
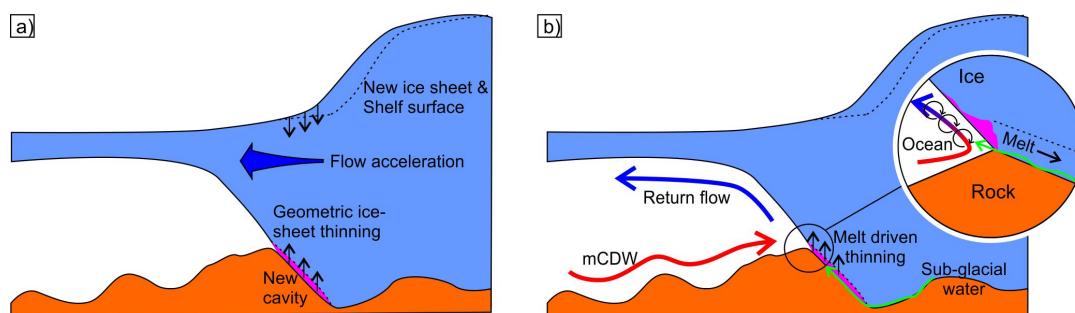
Figure 6: Conceptual models of grounding line retreat. a) Geometric thinning. b) Enhanced grounding line melting.
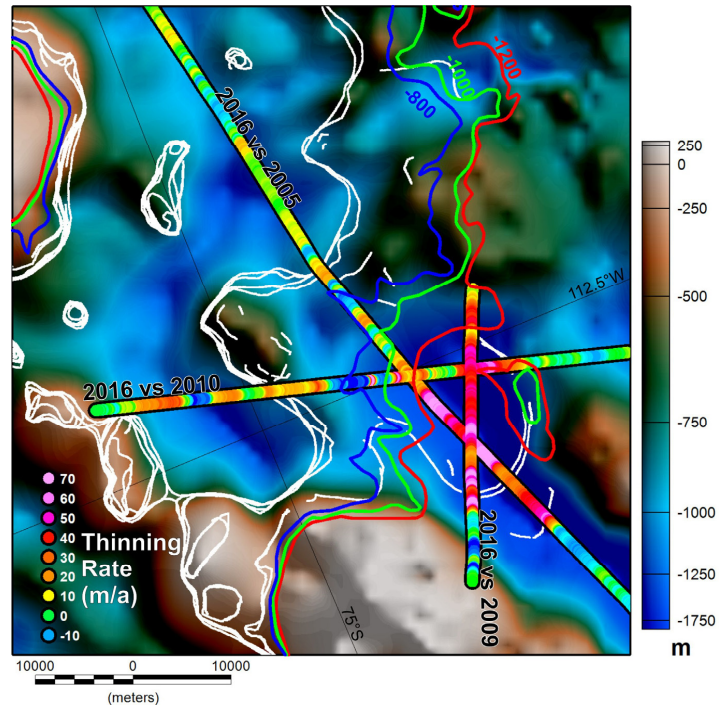
Figure 7: Rate of Crosson Ice Shelf thinning determined by direct radio-echo sounding measurements from 2009, 2010, and 2016
540 **OIB (Paden et al., 2010, updated 2018) and the 2005 AGASEA survey (Khazendar et al., 2016;Holt et al., 2006;Blankenship et al., 2012). Coloured contours show expected depth of base of floating ice shelf. White lines show INSAR derived grounding lines marking the front and back edges of the 'new' ice shelf (Rignot et al., 2014).**